^{11}C-Methionine PET of Acute Myocardial Infarction

Miyako Morooka[1], Kazuo Kubota[1], Hiromu Kadowaki[2], Kimiteru Ito[1], Osamu Okazaki[2], Mitsuo Kashida[2], Takuya Mitsumoto[1], Ren Iwata[3], Kuni Ohtomo[4], and Michiaki Hiroe[2]

[1]Division of Nuclear Medicine, Department of Radiology, International Medical Center of Japan, Tokyo, Japan; [2]Department of Cardiology, International Medical Center of Japan, Tokyo, Japan; [3]Department of Radiopharmaceutical Chemistry, Cyclotron Radioisotope Center, Tohoku University, Sendai, Miyagi, Japan; and [4]Department of Radiology, University of Tokyo, Tokyo, Japan

Tissue uptake of L-[methyl-^{11}C]-methionine (^{11}C-methionine) has been used to monitor amino acid metabolism and protein synthesis. We examined whether ^{11}C-methionine was retained in areas of myocardial infarction after successful reperfusion. **Methods:** Nine patients with infarction in the left anterior descendent region underwent percutaneous transluminal coronary artery intervention within 24 h and ^{201}Tl SPECT, ^{18}F-FDG PET, and ^{11}C-methionine PET within 2 wk of infarction onset. The standardized uptake values of the infarcted area and of the normal area were measured. **Results:** The ^{11}C-methionine images showed increased uptake in the infarcted area, whereas the ^{201}Tl SPECT and ^{18}F-FDG PET images showed decreased uptake. The highest accumulation of ^{11}C-methionine in the infarcted area was observed during the early phase of AMI. **Conclusion:** ^{11}C-methionine uptake is elevated in infarcted areas and may reflect the early acute phase of damage healing, that is, the initial process of remodeling.

Key Words: ^{11}C-methionine; myocardial infarction; PET; ^{18}F-FDG; remodeling

J Nucl Med 2009; 50:1283–1287
DOI: 10.2967/jnumed.108.061341

Labeled amino acids such as L-[methyl-^{11}C] methionine (^{11}C-methionine) have been used mainly for the diagnosis of brain and other tumors (*1–4*). ^{11}C-methionine uptake reflects not only protein synthesis but also amino acid transport and transmethylation (*2*). Several reports on cerebral infarction and gliomas have suggested a relation between ^{11}C-methionine uptake and angiogenesis (*4–6*). However, few studies have examined ^{11}C-methionine uptake in the myocardium since Barrio et al. first reported the use of various amino acids labeled with ^{13}N and ^{11}C-labeled L-amino acids about 25 y ago (*7*); in their report, they demonstrated a higher retention in ischemic segments than in control segments in a dog model of ischemia and reperfusion.

Received Dec. 17, 2008; revision accepted May 7, 2009.
For correspondence or reprints contact: Kazuo Kubota, International Medical Center of Japan, 1-21-1 Toyama, Shinjuku-ku, Tokyo, 162-8655 Japan.
E-mail: kkubota@imcj.hosp.go.jp or kkubota@cpost.plala.or.jp

The purpose of this study was to investigate whether ^{11}C-methionine accumulates in infarcted areas after successful reperfusion. We hypothesized that ^{11}C-methionine uptake might occur in infarcted areas after reperfusion and might reflect the early acute phase of damage healing, that is, the initial process of remodeling.

MATERIALS AND METHODS

Subjects and Study Protocol

The study protocol was approved by the Institutional Review Board, and written informed consent was obtained from each patient on entry into the study. The subjects consisted of 9 patients with acute myocardial infarction (AMI) in the anterior or anteroseptal wall who had undergone a percutaneous transluminal coronary artery intervention resulting in successful revascularization within 24 h after AMI onset. All patients underwent ^{201}Tl SPECT (mean day, 3.9), ^{18}F-FDG (7.2), and ^{11}C-methionine PET (6.6) within 2 wk of AMI onset. In addition, to enable a preliminary evaluation of the time course, we also evaluated 2 patients who had undergone follow-up studies at 3 or 6 mo after AMI onset.

^{201}Tl SPECT

We performed ^{201}Tl SPECT within 1 wk after a successful percutaneous transluminal coronary artery intervention. The patients were intravenously injected with 111 MBq of ^{201}Tl. One hour after the injection, myocardial SPECT images were obtained using a digital γ-camera and low-energy high-resolution collimators (ECAM; Siemens) according to the standard protocol.

^{18}F-FDG PET

After 6 h of fasting, the patients were orally given 75 g of glucose and their blood glucose level was measured 1 h later; ^{18}F-FDG (370 MBq) was then injected intravenously. If an elevated blood glucose level was observed, regular insulin was injected according to the guidelines of the American Society of Nuclear Cardiology (*8*). One hour after ^{18}F-FDG injection, PET/CT (Biograph 16; Siemens) of the heart was performed with a 7-min emission scan per bed position (1 bed position covered a 16-cm field of view along the *z*-axis) and CT attenuation correction. PET data were reconstructed with an ordered-subset expectation maximization algorithm (3 iterations, 8 subsets) using a Hanning filter.

^{11}C-Methionine PET

^{11}C-methionine was synthesized by the reaction of ^{11}C-methyltriflate with an aqueous solution of L-homocysteine thio-

lactone on a Sep-Pak tC18 cartridge (Waters) followed by purification with ion exchange cartridges (*9*). The radiochemical purity of the ^{11}C-methionine was more than 99%, and its clinical use was approved by the Institutional Review Board.

After 6 h of fasting, the patients were intravenously injected with 370 MBq of ^{11}C-methionine. Twenty minutes after injection, PET/CT of the heart was performed with an 8-min emission scan per bed position and CT attenuation correction. The reconstruction of the PET data was the same as that used for ^{18}F-FDG PET.

Before the patients had been examined, 3 healthy volunteers (2 men and 1 woman) were examined to determine the optimal timing of myocardial imaging after ^{11}C-methionine injection; dynamic data was acquired for up to 60 min after ^{11}C-methionine injection, and PET images of ^{11}C-methionine uptake in normal myocardium were thus obtained (Fig. 1A). In the normal myocardium, ^{11}C-methionine uptake was almost homogeneous, with a tendency toward a slight elevation in the basal anteroseptal area. In 2 volunteers, the average standardized uptake values (SUVs) of the basal anterior wall were 2.0 and 1.96 and those of the lateral wall were 1.71 and 1.78; the ratios of uptake in the basal anterior wall to the lateral wall were 1.17 and 1.10. Physiologic uptake in the liver was high, and this uptake masked some segments of the inferior wall. Patients with inferior-wall myocardial infarctions were also examined but were not included in the present study; instead, only cases of left anterior descendent infarction were chosen.

Analysis of SPECT and PET Images

First, we visually assessed uptake of the 3 tracers semiquantitatively by categorizing the regional uptake as greater than, less than, or similar to uptake in normal cardiac tissue. Next, to analyze ^{18}F-FDG and ^{11}C-methionine uptake in the PET images quantitatively, we determined the average SUVs of infarcted areas (infarction SUVs) and normal areas (normal SUVs) by placing regions of interest at corresponding places on short axial and long vertical views. The lateral wall was defined as a normal area, since stenosis of the coronary artery was not apparent on coronary angiography in any patient. The mean infarction and normal SUVs were calculated from 3 regions of interest in each area. The infarction-to-normal SUV ratio was also calculated. For ^{201}Tl, the average counts per pixel were determined in the infarction and normal zones, and the infarction-to-normal count ratio was calculated. All data were presented as the mean ± SD, and statistical differences were examined using an unpaired *t* test.

RESULTS

^{201}Tl and ^{18}F-FDG uptake was decreased, whereas ^{11}C-methionine uptake was similar or increased, relative to the normal region on semiquantitative visual analysis (Table 1). Table 1 summarizes the clinical information and analyzed data of the 9 patients (mean age, 57.1 ± 15.1 y; female-to-male ratio, 0:9). All infarction-to-normal count ratios were lower than 1.0 in the ^{201}Tl images. All infarction SUVs were lower than normal SUVs in the ^{18}F-FDG images, whereas all infarction SUVs were similar to or higher than normal SUVs in the ^{11}C-methionine images. Using the SUVs for all 9 patients, we determined the infarction-to-normal SUV ratio (mean ± SD) to be 0.39 ± 0.128 for the ^{18}F-FDG images and 1.207 ± 0.095 for the ^{11}C-methionine images (Fig. 1B). Representative patients are shown in

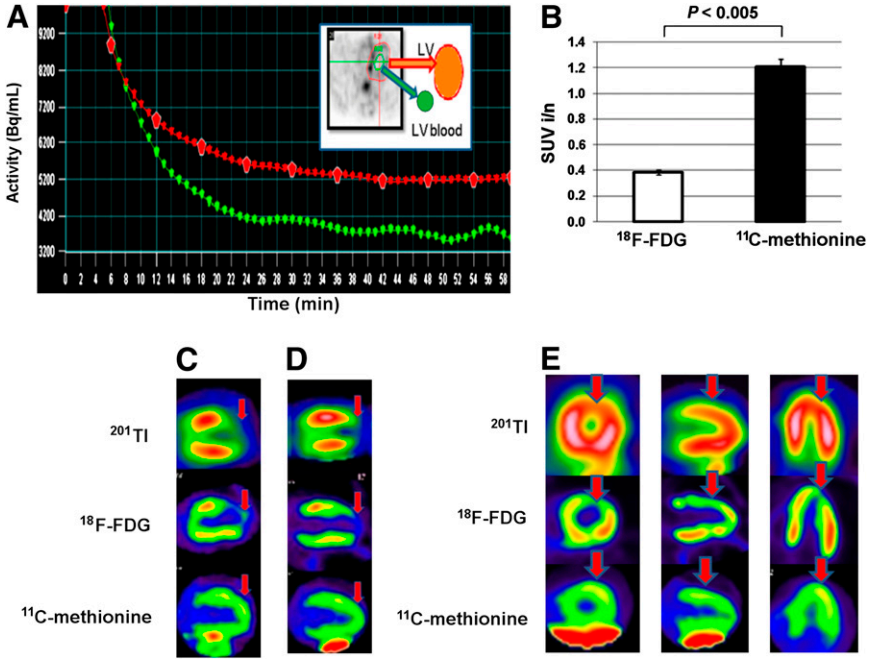

FIGURE 1. (A) Time–activity curves of regions of interest after tracer administration: whole left ventricle (red) and left ventricular blood pool (green). Blood-pool activity decreased from initially steep curve to stable lower level at around 20 min after injection, resulting in higher and stable myocardium–to–left-ventricle contrast at 20 min and thereafter. Then, we determined imaging time of myocardium with ^{11}C-methionine at 20 min after injection. (B) Comparison of infarction-to-normal SUV ratios (SUV i/n) on ^{18}F-FDG and ^{11}C-methionine images ($P < 0.005$ vs. ^{11}C-methionine imaging: mean ± SD, unpaired *t* test). (C and D) ^{201}Tl SPECT, ^{18}F-FDG PET, and ^{11}C-methionine PET in 53-y-old man (patient 7) (C) and 71-y-old man (patient 9) (D). In ^{11}C-methionine images, physiologic uptake in liver was high. Infarction zone in anterior wall exhibited decreased uptake on ^{201}Tl and ^{18}F-FDG images and increased uptake on ^{11}C-methionine images. ^{11}C-methionine uptake increased more in middle anterior wall than in apex: highest zone of uptake was almost next to spare zone in ^{201}Tl and ^{18}F-FDG images. ^{201}Tl images were similar to ^{18}F-FDG images visually. However, direct comparisons are difficult because of the different modalities. (E) Another instance of 3 orthogonal views of patient with segment 9 AMI (patient 8). Relative increase in ^{11}C-methionine uptake is also apparent in this patient.

TABLE 1. Clinical Information and Quantitative Data of Patients

Patient no.	Age (y)	Reperfusion Time* (h)	Segment no.	Risk factor	Peak CK (IU/L)	WBC (/μL)	^{201}Tl Day†	^{201}Tl Uptake‡	^{201}Tl Ratio¶	^{18}F-FDG Day†	^{18}F-FDG Uptake‡	^{18}F-FDG SUV Infarction	^{18}F-FDG SUV Normal	^{18}F-FDG SUV Ratio§	^{11}C-Methionine Day†	^{11}C-Methionine Uptake‡	^{11}C-Methionine SUV Infarction	^{11}C-Methionine SUV Normal	^{11}C-Methionine SUV Ratio§
1	40	2.5	7	HT	3,406	13,700	4	↓	0.52	6	↓	1.81	6.78	0.27	4	→	2.03	1.7	1.19
2	58	3	7	SM	4,764	9,200	5	↓	0.40	8	↓	2.05	6.73	0.31	4	→	1.69	1.36	1.24
3	60	13	6	SM	2,078	11,600	4	↓	0.45	4	↓	2.04	8.93	0.23	5	↑	2.62	2.33	1.12
4	73	6	7	SM	439	6,890	3	↓	0.71	8	↓	2.62	4.76	0.55	7	↑	2.63	1.93	1.36
5	63	24	7	HL, DM, SM	6,964	12,600	2	↓	0.38	10	↓	2.95	6.17	0.48	7	↑	2.13	1.65	1.29
6	53	6	6	HL, SM	3,468	12,230	2	↓	0.54	7	↓	2.08	5.43	0.38	8	↑	2.49	1.94	1.28
7	53	4.5	6	DM, SM	5,452	21,450	3	↓	0.70	7	↓	1.5	4.07	0.37	8	↑	2.26	2.06	1.10
8	43	12	9	HT, HL, SM	1,237	10,600	5	↓	0.70	9	↓	3.51	5.85	0.6	8	→	2.87	2.63	1.09
9	71	24	6	HT, DM, SM	1,324	11,900	7	↓	0.78	6	↓	1.78	5.42	0.33	8	↑	2.9	2.47	1.17
Mean					3,232	12,241	3.9		0.58	7.2		2.26	6.02	0.39	6.6		2.40	2.01	1.21
SD					2,180.7	402.6			0.15			0.64	1.40	0.13			0.41	0.41	0.10

*Interval between onset of acute symptoms and beginning of reperfusion.
†Day scanning was performed after AMI onset.
‡Visual uptake in infarcted area compared with normal area: → = similar; ↑ = increased; ↓ = decreased.
¶Infarction-to-normal count activity ratio.
§Infarction-to-normal SUV ratio.
CK = creatine kinase; WBC = white blood cell count; HT = hypertension; SM = smoking; HL = hyperlipidemia; DM = diabetes.

Figures 1C–1E. Two patients with segment 6 AMI (Figs. 1C and 1D) exhibited increased uptake of ^{11}C-methionine in the infarct zone, although uptake of the other tracers was decreased in the same zone. The greatest ^{11}C-methionine uptake was not in the core of the infarct region but in the border region between the infarct and normal tissue. Visually, relative ^{18}F-FDG uptake was reduced in the infarction zone, and the ^{201}Tl uptake was the same. Three orthogonal views of another patient with no. 9 AMI are shown in Figure 1E. A relative increase in ^{11}C-methionine uptake is visible. Figure 2 shows the changes in ^{11}C-methionine uptake in studies performed 1 wk and 3 mo (patient 3) and 6 mo (patient 7) after AMI onset. At 3 mo after onset, uptake of ^{11}C-methionine was similar to that observed during the acute phase, whereas uptake was decreased or showed a partial defect at 6 mo after onset. The ^{11}C-methionine infarction-to-normal SUV ratio also decreased in 2 patients (Table 1). Thus, ^{11}C-methionine uptake changed during imaging studies performed over the course of 6 mo after AMI onset.

DISCUSSION

^{11}C-methionine PET has been used for diagnosing brain tumors and evaluating their treatment (*1–4*). Because of the low physiologic uptake of ^{11}C-methionine in the brain, ^{11}C-methionine PET is currently used mainly to assess brain tumors. Numerous studies have examined ^{11}C-methionine uptake, and ^{11}C-methionine uptake is widely known to reflect amino acid transport, transmethylation, and protein synthesis. In particular, Ishiwata et al. reported that the amino acid transport system was dominant in the brain and in tumors (*2*). Kracht et al. demonstrated a correlation between ^{11}C-methionine uptake and microvessel density and showed a strong correlation between increased amino acid uptake and angiogenesis in evolving gliomas (*4*). In studies on brain infarction, Jacobs observed an increase in ^{11}C-methionine uptake in peripheral areas of acute cerebral infarction (*5*), and Nagano-Saito et al. concluded that ^{11}C-methionine uptake by damaged but viable brain tissue represented gliosis and angiogenesis (*6*).

However, few studies have examined the application of ^{11}C-methionine PET to myocardial imaging, especially using clinical PET images. Here, we presented ^{201}Tl SPECT and ^{18}F-FDG/^{11}C-methionine PET images of AMI after successful reperfusion. All the ^{201}Tl and ^{18}F-FDG images were typical of myocardial ischemia and exhibited similar uptake profiles. However, the ^{11}C-methionine images showed a different pattern of uptake. An increase in ^{11}C-methionine uptake was observed in regions exhibiting reduced or the absence of ^{201}Tl and ^{18}F-FDG uptake.

As we had suspected on the basis of the pattern of ^{11}C-methionine uptake in the brain, ^{11}C-methionine uptake was observed in regions of myocardial infarction. Blankesteijn et al. separated the process of healing after myocardial infarction into 4 phases: myocardial cell death, acute inflammation, the formation of granulation tissue, and scar

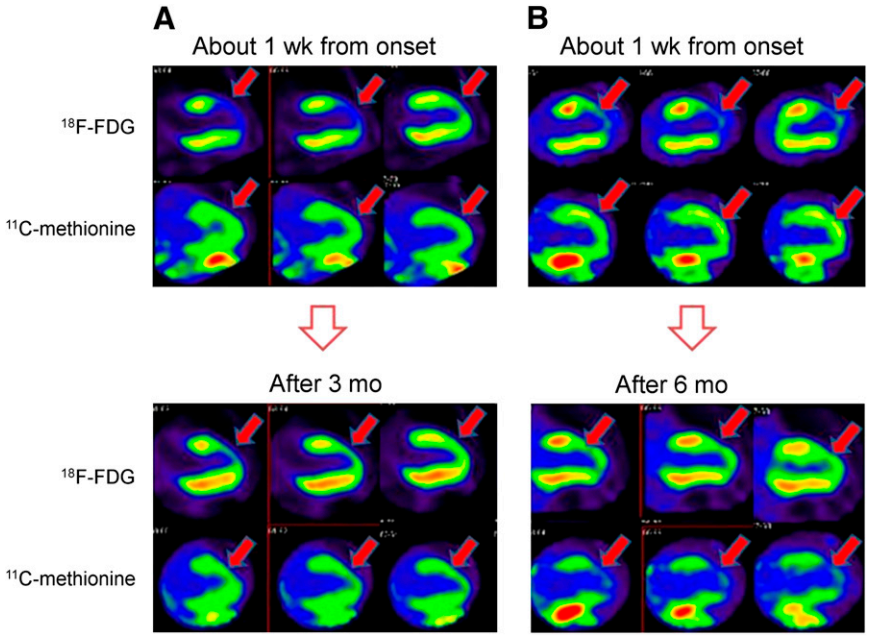

FIGURE 2. Vertical long-axis images obtained 1 wk and 3 mo after AMI onset in 60-y-old man (patient 3) (A) and 1 wk and 6 mo after AMI onset in 53-y-old man (patient 7) (B). In both patients, ^{11}C-methionine uptake in region was higher than that in lateral wall at 1 wk after AMI onset (infarction-to-normal ratios, 1.12 and 1.10). However, uptake became similar to ^{18}F-FDG uptake at 3 mo after AMI onset and almost undetectable after 6 mo (infarction-to-normal ratios, 0.80 and 0.77). Uptake was slightly increased around infarction zone in ^{18}F-FDG images obtained at 3 mo after AMI onset, whereas decreased ^{18}F-FDG uptake was observed at 6 mo.

formation (*10*). ^{11}C-methionine uptake was observed in the second and third of these phases.

During the acute inflammatory reactions that occur during the early phase of healing, many inflammatory cells in the damaged region produce cytokines, which degrade the extracellular collagen matrix (*11*). In tumor tissue, ^{11}C-methionine uptake increases in granulation tissue and macrophages, but not as much as does ^{18}F-FDG (*1*). Thus, ^{11}C-methionine uptake may reflect the activity of these inflammatory cells.

On the other hand, numerous small blood vessels are present during the formation of granulation tissue. Angiogenesis, a repair process after ischemic injuries (*12*), recently has become a field of molecular imaging research (*13–17*). ^{111}In-RP748 SPECT (*13*) and ^{18}F-galacto-RGD PET (*14*) targeting $\alpha_v\beta_3$ integrin, an angiogenic factor, have been used to study animal models of myocardial infarction; these studies showed overexpression of $\alpha_v\beta_3$ integrin in activated endothelial cells during angiogenesis after hypoxia, and increased uptake was observed in infarcted areas. The time course of the ^{11}C-methionine images obtained after AMI was similar to the acute phase of angiogenesis described in these reports. Thus, the increased uptake of ^{11}C-methionine might reflect some angiogenic factors, as mentioned in the above studies on cerebral infarction and gliomas, suggesting a relation between ^{11}C-methionine uptake and angiogenesis. Possibly, the amino acid transport system might become active during remodeling of the heart, just as it does in the brain and in tumors.

This study had some limitations. ^{11}C-methionine uptake was elevated during early AMI. This elevated uptake may gradually decrease until it disappears in scar tissue. ^{11}C-methionine uptake after infarction may be useful for assessing the process of remodeling after AMI and for monitoring the effects of therapy. Further studies on ^{11}C-methionine uptake after myocardial infarction are needed.

The present findings were limited to only the early acute phase of myocardial infarction, and more data on long-term changes in ^{11}C-methionine uptake should be obtained.

In addition, although we compared ^{201}Tl uptake for perfusion images, ^{18}F-FDG for glucose metabolism, and ^{11}C-methionine for amino acid metabolism, differences between the SPECT and PET modalities prevented us from determining whether the region of ^{11}C-methionine uptake better matched the region of low ^{18}F-FDG uptake or the region of ^{201}Tl hypoperfusion.

Furthermore, because our ^{18}F-FDG PET images were obtained after the oral administration of glucose, a comparison of ^{18}F-FDG after fasting with heparin injection and ^{11}C-methionine uptake would be useful to confirm whether ^{11}C-methionine uptake actually reflects acute inflammation or ischemia.

Finally, from a technical viewpoint, the considerable physiologic uptake of ^{11}C-methionine in the liver makes a detailed assessment of the right coronary artery area difficult.

CONCLUSION

We have presented the first (to our knowledge) images of ^{11}C-methionine uptake in damaged myocardium after reperfusion for AMI. These images differ greatly from those of ^{201}Tl and ^{18}F-FDG uptake. ^{11}C-methionine uptake might reflect an aspect of dynamic myocardial changes, such as remodeling during healing, after reperfusion for AMI.

ACKNOWLEDGMENTS

We thank Drs. Yuriko Tanaka, Hiroyuki Soejima, Yuiichi Tamori, Munehiro Kamimura, Tomohiro Yamazaki, Junko Shibata, Kazuhiko Nakajima, and Ai Hori. Part of this study was supported by Grant-in-Aid 17-12 for cancer research from the Ministry of Health, Labor, and Welfare.

REFERENCES

1. Kubota R, Kubota K, Yamada S, et al. Methionine uptake by tumor tissue: a microautoradiographic comparison with FDG. *J Nucl Med.* 1995;36:484–492.
2. Ishiwata K, Kubota K, Murakami M, et al. Re-evaluation of amino acid PET studies: can the protein synthesis rates in brain and tumor tissues be measured in vivo? *J Nucl Med.* 1993;34:1936–1943.
3. Kubota K. From tumor biology to clinical PET: a review of positron emission tomography (PET) in oncology. *Ann Nucl Med.* 2001;15:471–486.
4. Kracht LW, Friese M, Herholz K, et al. Methyl-[^{11}C]-L-methionine uptake as measured by positron emission tomography correlates to microvessel density in patients with glioma. *Eur J Nucl Med Mol Imaging.* 2003;30:868–873.
5. Jacobs A. Amino acid uptake in ischemically compromised brain tissue. *Stroke.* 1995;26:1859–1866.
6. Nagano-Saito A, Kato T, Wakabayashi T, et al. High- and moderately high-methionine uptake demonstrated by PET in a patient with a subacute cerebral infarction. *Ann Nucl Med.* 2001;15:387–391.
7. Barrio JR, Baumgartner FJ, Henze E, et al. Synthesis and myocardial kinetics of N-13 and C-11 labeled branched chain L-amino acids. *J Nucl Med.* 1983; 24:937–944.
8. Bacharach SL, Bax JJ, Case J, et al. PET myocardial glucose metabolism and perfusion imaging: part I—guidelines for patient preparation and data acquisition. *J Nucl Cardiol.* 2003;10:543–554.
9. Watanabe T, Iwata R, Ishikawa Y, Sato T, Ishiwata K. Development of a miniature module for on-column preparation of [C-11]methionine from [C-11]methyl triflate. In: Abstracts of the 9th Congress of the World Federation of Nuclear Medicine and Biology; Oct. 22–27, 2006; Seoul, Korea. No. 3003, S93.
10. Blankesteijn WM, Creemers E, Lutgens E, Cleutjens JP, Daemen MJ, Smits JF. Dynamics of cardiac wound healing following myocardial infarction: observations in genetically altered mice. *Acta Physiol Scand.* 2001;173:75–82.
11. Jugdutt BI. Ventricular remodeling after infarction and the extracellular collagen matrix: when is enough enough? *Circulation.* 2003;108:1395–1403.
12. Khurana R, Simons M, Martin JF, Zachary IC. Role of angiogenesis in cardiovascular disease: a critical appraisal. *Circulation.* 2005;112:1813–1824.
13. Meoli DF, Sadeghi MM, Krassilnikova S, et al. Noninvasive imaging of myocardial angiogenesis following experimental myocardial infarction. *J Clin Invest.* 2004;113:1684–1691.
14. Higuchi T, Bengel FM, Seidl S, et al. Assessment of αvβ3 integrin expression after myocardial infarction by positron emission tomography. *Cardiovasc Res.* 2008;78:395–403.
15. Haubner R, Weber WA, Beer AJ, et al. Noninvasive visualization of the activated alphavbeta3 integrin in cancer patients by positron emission tomography and [^{18}F]galacto-RGD. *PLoS Med.* 2005;2:e70.
16. Beer AJ, Haubner R, Goebel M, et al. Biodistribution and pharmacokinetics of the αvβ3-selective tracer ^{18}F-galacto-RGD in cancer patients. *J Nucl Med.* 2005;46:1333–1341.
17. Hua J, Dobrucki LW, Sadeghi MM, et al. Noninvasive imaging of angiogenesis with a ^{99m}Tc-labelled peptide targeted at alphavbeta3 integrin after murine hindlimb ischemia. *Circulation.* 2005;111:3255–3260.

JNM The Journal of NUCLEAR MEDICINE

^{11}C-Methionine PET of Acute Myocardial Infarction

Miyako Morooka, Kazuo Kubota, Hiromu Kadowaki, Kimiteru Ito, Osamu Okazaki, Mitsuo Kashida, Takuya Mitsumoto, Ren Iwata, Kuni Ohtomo and Michiaki Hiroe

J Nucl Med. 2009;50:1283-1287.
Published online: July 17, 2009.
Doi: 10.2967/jnumed.108.061341

The Journal of Nuclear Medicine is published monthly.
SNMMI | Society of Nuclear Medicine and Molecular Imaging
1850 Samuel Morse Drive, Reston, VA 20190.
(Print ISSN: 0161-5505, Online ISSN: 2159-662X)

SNMMI SOCIETY OF NUCLEAR MEDICINE AND MOLECULAR IMAGING